Kinetic analysis of the thermal isomerisation pathways in an asymmetric double azobenzene switch

Robertus, Jort; Reker, Siebren F.; Pijper, Thomas C.; Deuzeman, Albert; Browne, Wesley R.; Feringa, Ben L.

Published in:
Physical Chemistry Chemical Physics

DOI:
10.1039/c2cp23756c

Publication date:
2012

Electronic Supplementary Material (ESI) for Physical Chemistry Chemical Physics

Supporting Information

Kinetic analysis of the thermal isomerisation pathways in an asymmetric double azobenzene switch

Jort Robertus,[a] Siebren F. Reker,[c] Thomas C. Pijper,[b] Albert Deuzeman,[c] Wesley R. Browne[a, b] and Ben L. Feringa*[a, b]*

[a] *Stratingh Institute for Chemistry, Nijenborgh 4, 9747 AG, Groningen, The Netherlands.*
[b] *Zernike Institute for Advanced Materials, Nijenborgh 4, 9747 AG, Groningen, The Netherlands.*
[c] *Centre for Theoretical Physics, Nijenborgh 4, 9747 AG, Groningen, The Netherlands. Tel: +31 50 363 3420*

e-mail: w.r.browne@rug.nl, b.l.feringa@rug.nl

1. Experimental section

1.1 General remarks

For synthesis all chemicals were obtained from commercial sources and used as received unless stated otherwise. Solvents were reagent grade. For column chromatography, silica gel (Silicycle Siliaflash P60, 40-63 μm, 230-400 mesh) was used in all cases. Separation was determined on Merck TLC silica gel 60, kieselguhr F_{254}. ^{1}H and ^{13}C NMR spectra were recorded on a Varian Gemini-200 (operating at 200 and 50 MHz), a Varian VXR-300 (operating at 300 and 75 MHz) and a Varian AMX400 (operating at 400 and 100 MHz) spectrometer. Kinetic and temperature dependant ^{1}H-NMR studies were recorded on a Varian Unity Plus (500 MHZ) in CD_2Cl_2, $C_2D_4Cl_2$ and DMSO-d_6. Chemical shifts are reported in δ values (ppm) relative to $CDCl_3$ (^{1}H δ = 7.24, ^{13}C δ = 77.2), CD_2Cl_2 (^{1}H δ = 5.32, ^{13}C δ = 54.0), $C_2D_4Cl_2$ (^{1}H δ = 3.72), and DMSO-d_6 (^{1}H δ = 2.50, ^{13}C δ = 39.5). For ^{1}H-NMR the signals were assigned as following: singlet (s), doublet (d), double doublet (dd), triplet (t), quartet (q), and multiplet (m). For ^{13}C-NMR, the signals were designated as: primary carbon (CH_3), secondary carbon (CH_2), tertiary carbon (CH), quaternary carbon (C). MS spectra were obtained on a Hewlett-Packard HP 6890 GC with HP 5973 mass selective detector, containing a Agilent 5%-(phenyl)methylpolysiloxane column (25 m × 0.25 mm × 0.25 μm). MS (ESI, APCI) and HRMS (ESI, APCI) spectra were obtained on a Thermo scientific LTQ Orbitrap XL. Melting points were recorded using a Buchi melting point B-545 apparatus. UV/Vis absorption spectra were recorded on a Hewlett-Packard HP 8453 FT spectrometer using Uvasol grade solvents. Irradiation experiments were performed with a spectroline ENBC-280C/FE UV lamp (365 nm) or an Innolas Spitlight 400 Nd;YAG laser (excitation at 355 nm, 10 Hz, 40 mW).

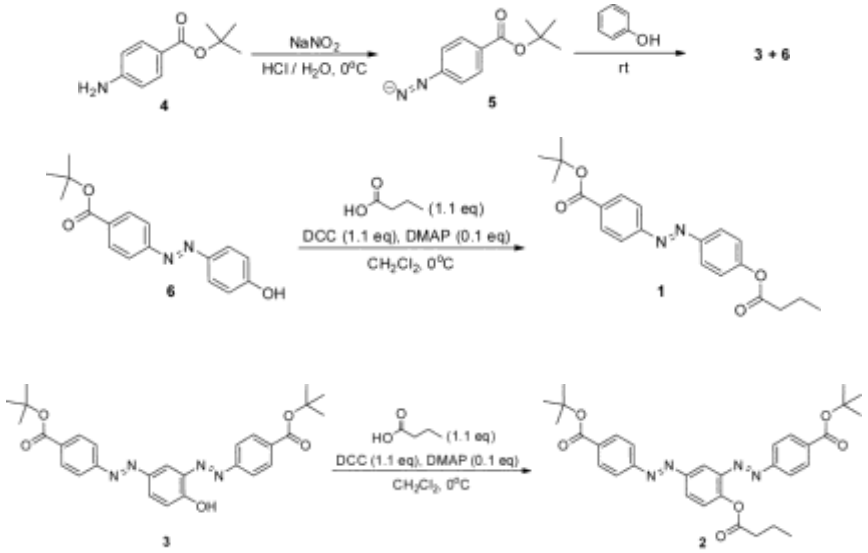

Fig. S1 Synthesis of phenol substituted azobenzene switches **3** and **6** and butanoate functionalized azobenzene switches **1** and **2**.

1.2 Synthesis of *tert*-butyl-4,4'-(1*E*,1'*E*)-(4-hydroxy-1,3-phenylene)bis(diazene-2,1-diyl)dibenzoate (3)

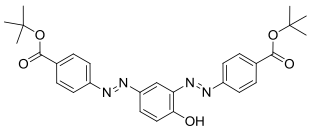

4-Aminobenzoic acid *tert*-butyl ester **4** (5.00 g, 26 mmol) was dissolved in a stirred aqueous solution of dilute hydrochloric acid (1 mM, 60 mL). The resulting solution was cooled to 0°C. Compound **3** was diazotized by a dropwise addition of 5 mL solution of $NaNO_2$ (1.79 g, 26 mmol) in water at 0 °C. Upon addition of $NaNO_2$, the solution became intensely yellow. The yellow solution was diluted with chilled methanol (100 mL), subsequently the coupling was performed by slow addition of the diazotized mixture to a mixture of phenol (2.35 g, 25 mmol), KOH (2.81 g, 50 mmol), and MeOH (25 mL) at 0°C. The mixture was neutralized with aqueous 10% HCl solution and subsequently extracted with ethyl acetate (3 × 150 mL). The combined organic layers were washed with brine (2 × 200 mL) and dried over Mg_2SO_4. The organic solvent was

removed under reduced pressure and an orange-red oil was obtained. The oil was dry loaded onto celite and purified by column chromatography (SiO_2, pentane / ethyl acetate = 4:1, R_f = 0.79). The excess of organic solvent was removed *in vacuo* to yield a red solid, which was recrystallized from *n*-hexane. Compound **3** was obtained as red crystals (1.17 g, 18 mmol, 9 %). m.p.: 141-142 °C. ^{1}H NMR (200 MHz, $CDCl_3$) δ 1.63 (s, 18H), 7.15 (d, *J* = 8.8 Hz, 1H), 7.92 (m, 4H), 8.04 (d, *J* = 8.8 Hz, 2H), 8.14 (m, 4H), 8.59 (s, 1H), 13.24 (s, 1H); ^{13}C NMR (100 MHz, $CDCl_3$) δ 28.4 (CH_3), 81.6 (C), 81.9 (C), 119.3 (CH), 122.3 (CH), 122.6 (CH), 127.9 (CH), 130.6 (CH), 130.9 (CH), 133.7 (C), 134.6 (C) 152.6 (C) 154.9 (C) 156.2 (C) 165.0 (C) 165.4 (C; *m/z* (APCI pos,) = 503 ($+H^+$) ; HRMS (EI): calcd. for $C_{28}H_{31}N_4O_5$ H^+: 503.2216 found 503.2289.

1.3 Synthesis of *tert*-butyl-4,4'-(1E,1'E)-(4-(butyryloxy)-1,3-phenylene)bis(diazene-2,1-diyl) dibenzoate (2)

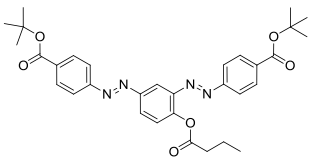

A solution of DCC (812 mg, 3.9 mmol) in DCM (2 mL) was added dropwise to a solution of **3** (789 mg, 1.6 mmol), butyric acid (277 mg, 0.3 mL, 3.1 mmol), and DMAP (46 mg, 0.4 mmol) in DCM (3 mL) at 0°C under an argon atmosphere. The reaction mixture was stirred for 20 min at 0°C. The colour of the reaction mixture changed from dark red to bright orange. Subsequently the solution was allowed to warm to rt and stirred for 1 h. The solvent was removed *in vacuo* and the orange solid obtained was further purified by column chromatography (SiO_2, pentane / ethyl acetate = 10:1, R_f = 0.44) to afford **2** as orange crystals (837 mg, 1.5 mmol, 93 %). m.p.: 146-147 °C. ^{1}H NMR (500 MHz, CD_2Cl_2) δ 1.05 (t, *J* = 7.3 Hz, 3H), 1.61 (s, 18H), 1.78-1.82 (m, 2H), 2.69 (t, *J* = 7.3 Hz, 2H), 7.42 (d, *J* = 8.6 Hz, 1H), 7.93 (dd, *J* = 7.8, 11.4 Hz, 4H), 8.12 (d, *J* = 9.3 Hz, 1H), 8.14 (d, *J* = 8.6 Hz, 1H) 8.30 (s, 1H); ^{13}C NMR (100 MHz, CD_2Cl_2) δ 14.2 (CH_3), 19.0 (CH_2), 28.5 (CH_3), 36.4 (CH_2), 81.9 (C), 82.0 (C), 112.2 (CH), 123.2 (CH), 123.3 (CH), 125.0 (CH) 127.2 (CH), 130.9 (CH), 134.9 (C), 135.2 (C), 145.2 (C), 151.1 (C), 152.2 (C), 155.1 (C), 155.3 (C), 165.3 (C), 165.4 (C), 172.3 (C); *m/z* (EI, %) = 573, (100); HRMS (EI): calcd. for $C_{32}H3_6N_4O_6$ + H: 573.2635, found 573.2716.

1.4 Synthesis of (E)-4-((4-hydroxyphenyl)diazenyl)benzoic acid (6)

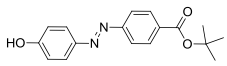

E-4-(4-hydroxyphenylazo)benzoic acid *tert*-butyl ester **6** was obtained during the synthesis of compound **3**. Compound **6** was purified using column chromatography (rf: SiO_2, pentane / ethyl acetate = 4:1, R_f = 0.57). The excess of organic solute was removed *in vacuo* and a red solid was obtained and recrystallized from *n*-hexane. Compound **6** was obtained as red crystals (5.22 g, 18 mmol, 68 %). m.p.: 145-146 °C. ^{1}H NMR (400 MHz, $CDCl_3$) δ 1.64 (s, 9H), 6.47 (s, 1H), 6.98 (d, *J* = 8.8 Hz, 2H), 7.89 (q, *J* = 1.8, 6.6 Hz, 4H), 8.12 (d, *J* = 8.4 Hz, 2H); ^{13}C NMR (100 MHz, $CDCl_3$) δ 28.4 (CH_3), 82.0 (C), 116.1 (CH), 122.6 (CH), 125.6 (CH), 130.6 (CH), 133.1 (C), 147.2 (C), 155.3 (C) 159.5 (C); *m/z* (APCI, pos) = 299; HRMS (APCI, pos): calcd. for $C_{17}H_{19}N_2O_3$ $+H^+$: 299.1317 found 299.1390.

1.5 Synthesis of *tert*-Butyl-4-((4-(5-(1,2-dithiolan-3-yl)pentanoyloxy)phenyl) diazenyl) benzoate (1)

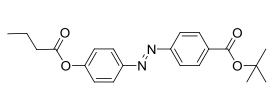

1 was synthesized as described for **2**, and purified by column chromatography (SiO_2, pentane: ethyl acetate = 4:1, R_f = 0.70) to afford **1** as orange crystals (55 mg, 0.14 mmol, 79 %). *(caution: butyric acid is extremely putrid)* m.p.: 101-102 °C. ^{1}H NMR (300 MHz, $CDCl_3$) δ1.10 (t, *J* = 7.3 Hz, 3H), 1.66 (s, 9H), 1.83-1.86 (m, 2H), 2.61 (t, *J* = 7.3 Hz, 2H), 7.29 (d, *J* = 8.8 Hz, 2H), 7.99 (dd, *J* = 8.4, 11.4 Hz, 4H), 8.17 (d, *J* = 8.4 Hz, 1H); ^{13}C NMR (100 MHz, $CDCl_3$) δ 13.9 (CH_3), 18.6 (CH_2), 28.4 (CH_3), 36.4 (CH_2), 81.6 (C), 122.5 (CH), 122.7 (CH), 130.6 (CH), 134.0 (C) 150.3 (C), 153.4 (C), 154.9 (CH), 165.3 (C), 171.9 (C); *m/z* (APCI, pos) = 299; HRMS (APCI, pos): calcd. for $C_{21}H_{24}N_2O_4$ $+H^+$: 369.1736 found 369.1789.

1.5 Photochemical *E* to *Z* isomerization

Samples used for arrayed ^{1}H-NMR experiments were prepared as following. A 1 ml solution of *E,E*-**1** (4×10^{-5} M in $C_2H_4Cl_2$, at 20°C) was irradiated at λ_{exc} 355 nm (10 Hz, 5-6 ns pulse, 30 mW) in a quartz cuvette (pathlength 1 mm) for 9 h. Thermal array ^{1}H-NMR experiments were carried out on a Varian Unity Plus (500 MHz).

Separation of the isomers was achieved by irradiating a sample containing *E,E*-**2** in 1 ml CH_2Cl_2 at 20°C, at λ_{exc} 355 nm in a stirred 1 ml quartz cuvette (d = 1 cm) for 9 h. The PSS mixture was subsequently applied to a Merck PLC plate (Silica gel 60, 3 mm, 20 × 20 cm) and eluted with pentane / ethylacetate, 10:1 (R_f: *E,E*-**2** = 0.44, *ortho-Z,E*-**2** = 0.33, *para-Z,E*-**2** = 0.20, *Z,Z*-**2** = 0.12).

1.6 Photochemical *Z* to *E* isomerization

The *Z* to *E* photo isomerization was performed by irradiating a PSS solution of **1** (2.50×10^{-5} M in CH_2Cl_2, at 20°C) at λ_{exc} 450 nm in a 1 cm quartz cuvette.

1.7 Thermal Z to E isomerization

Changes in the UV and ^{1}H-NMR spectra upon thermal reversion were determined by irradiating (λ_{exc} 355 nm) a sample of *E,E*-**2** (4×10^{-5} M in $C_2H_4Cl_2$, at 20°C) to the PSS as previously indicated. Subsequently the sample was heated at various temperatures in the Varian Unity Plus (500 MHZ) spectrometer ^{1}H-NMR experiments used Varian software (VNMRJ version 2.2 revision D 2008 inova).

2. Results and discussion

2.1 Structural characterization of *E*-6

The structure of *E*-**6** was elucidated using ^{1}H-NMR and ^{13}C spectroscopy.

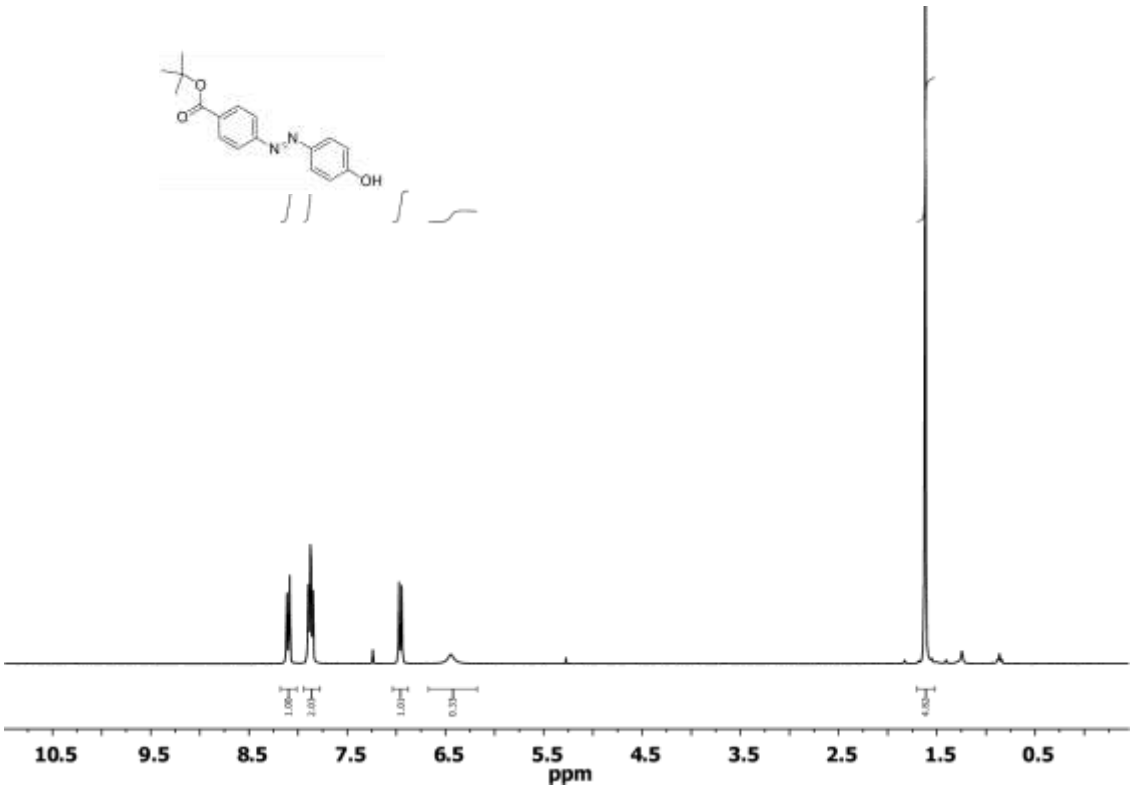

Fig. S2 ^{1}H-NMR spectrum of switch *E*-**6** in $CDCl_3$.

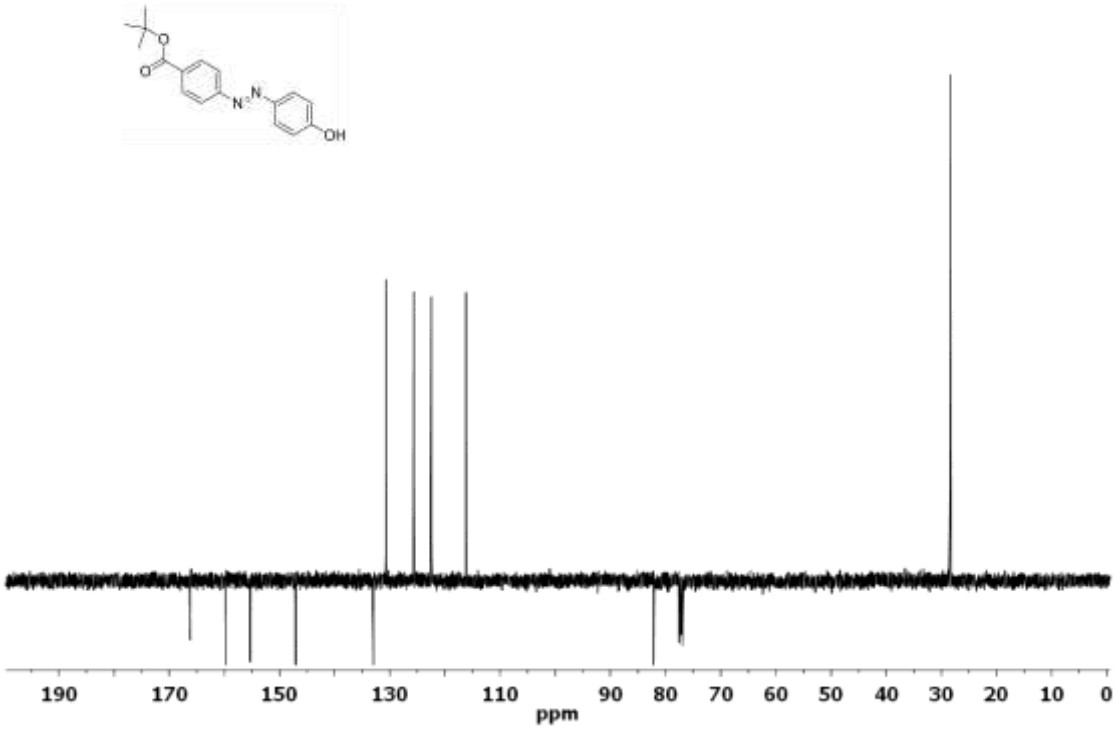

Fig. S3 APT ^{13}C-NMR spectrum of switch *E*-**6** in CD_2Cl_2.

2.2 Structural characterization of *E*-1

The structure of *E*-**1** was elucidated using ^{1}H-NMR, and ^{13}C spectroscopy.

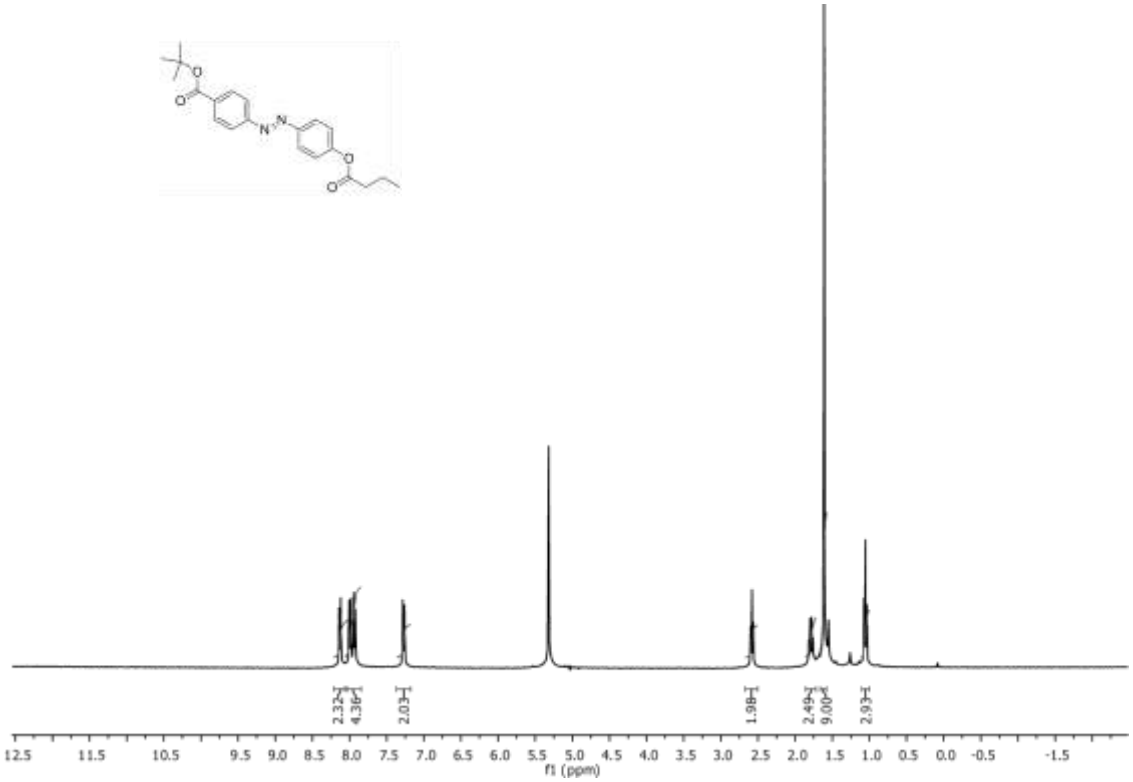

Fig. S4 ^{1}H-NMR spectrum of switch *E*-**1** in CD_2Cl_2.

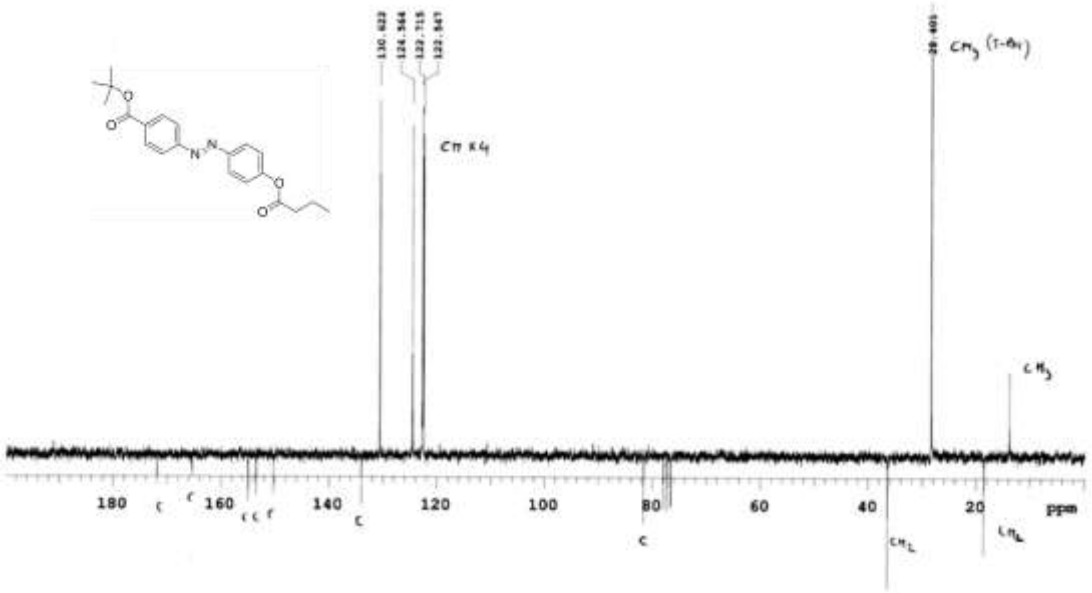

Fig. S5 APT ^{13}C-NMR spectrum of switch *E*-**1** in CD_2Cl_2.

2.3 Structural characterization of *E,E*-3

The structure of *E,E*-**3** was elucidated using ^{1}H-NMR, and ^{13}C spectroscopy.

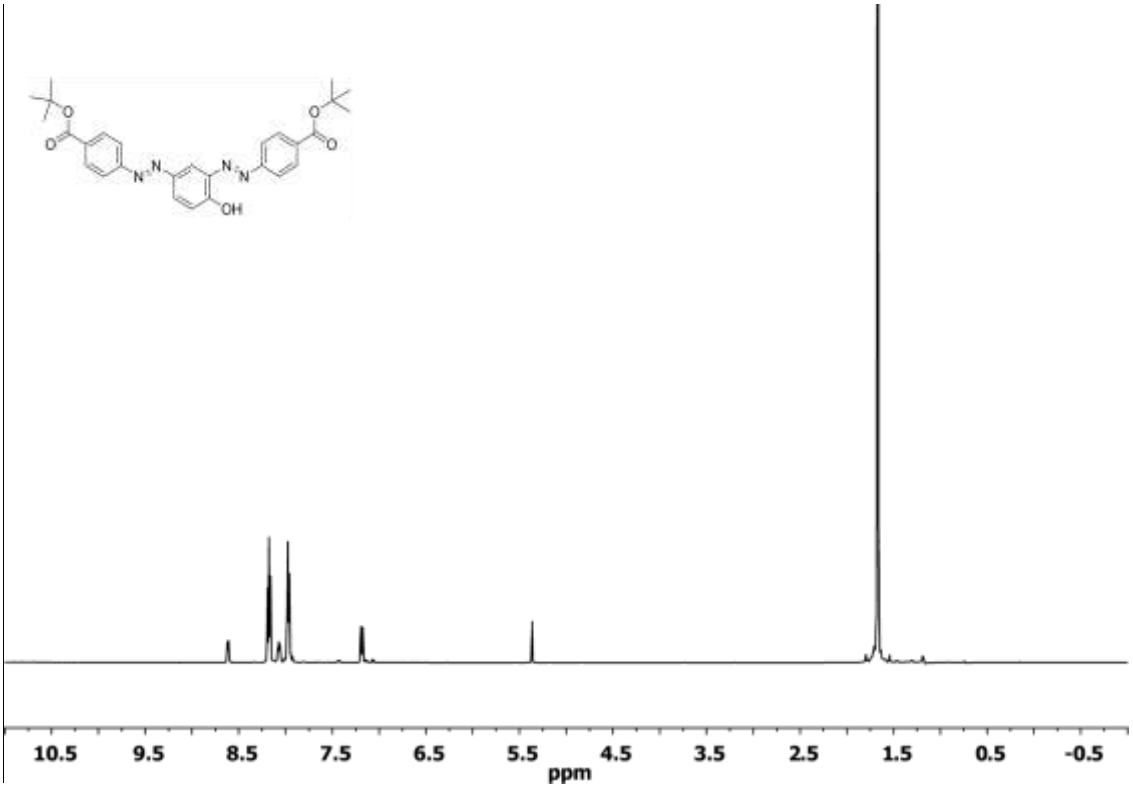

Fig. S6 ^{1}H-NMR spectrum of switch *E,E*-**3** in CD_2Cl_2.

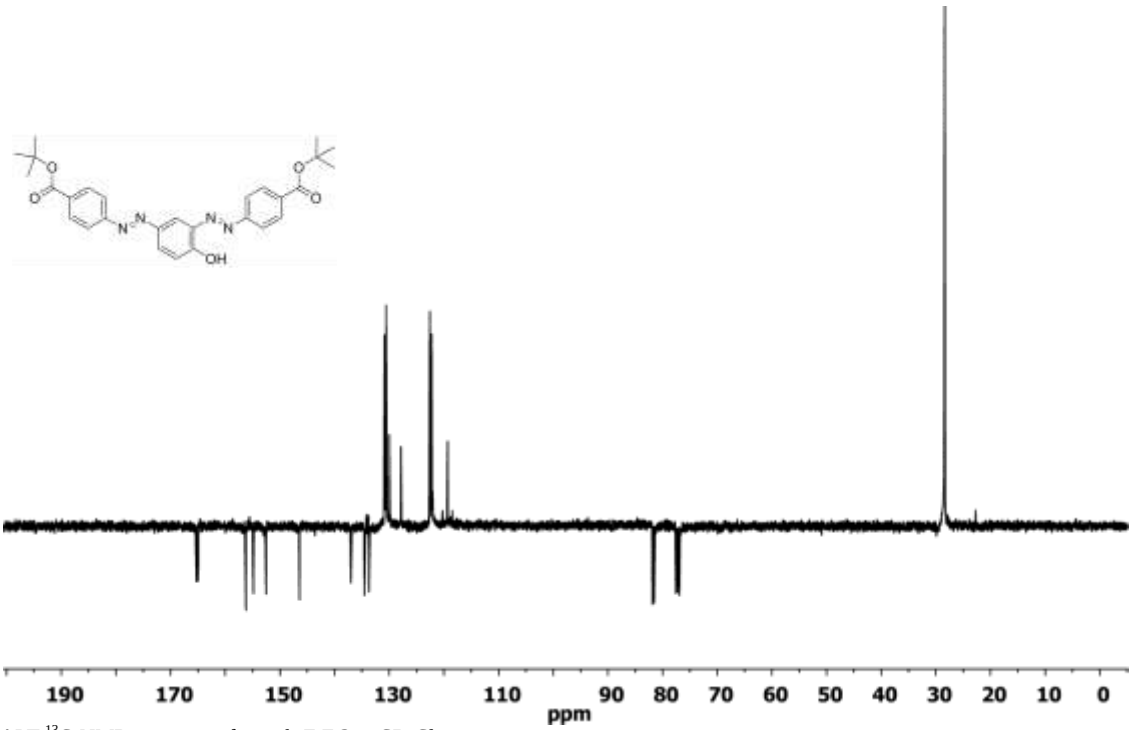

Fig. S7 APT ^{13}C-NMR spectrum of switch *E,E*-**3** in CD_2Cl_2.

2.4 Structural characterization of *E,E*-2

The structure of *E,E*-**2** was elucidated using ^{1}H-NMR, ^{13}C, GCOSY, HSQC and NOE-spectroscopy.

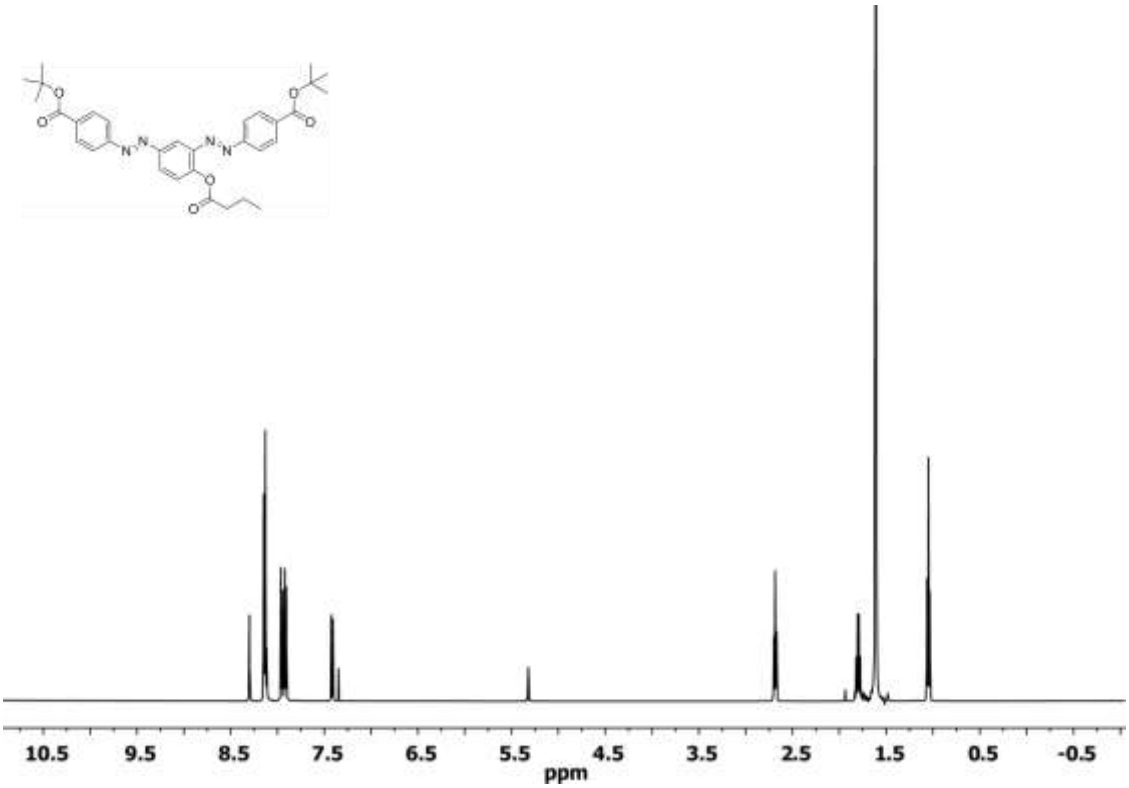

Fig. S8 ^{1}H-NMR spectrum of switch *E,E*-**2** in CD_2Cl_2.

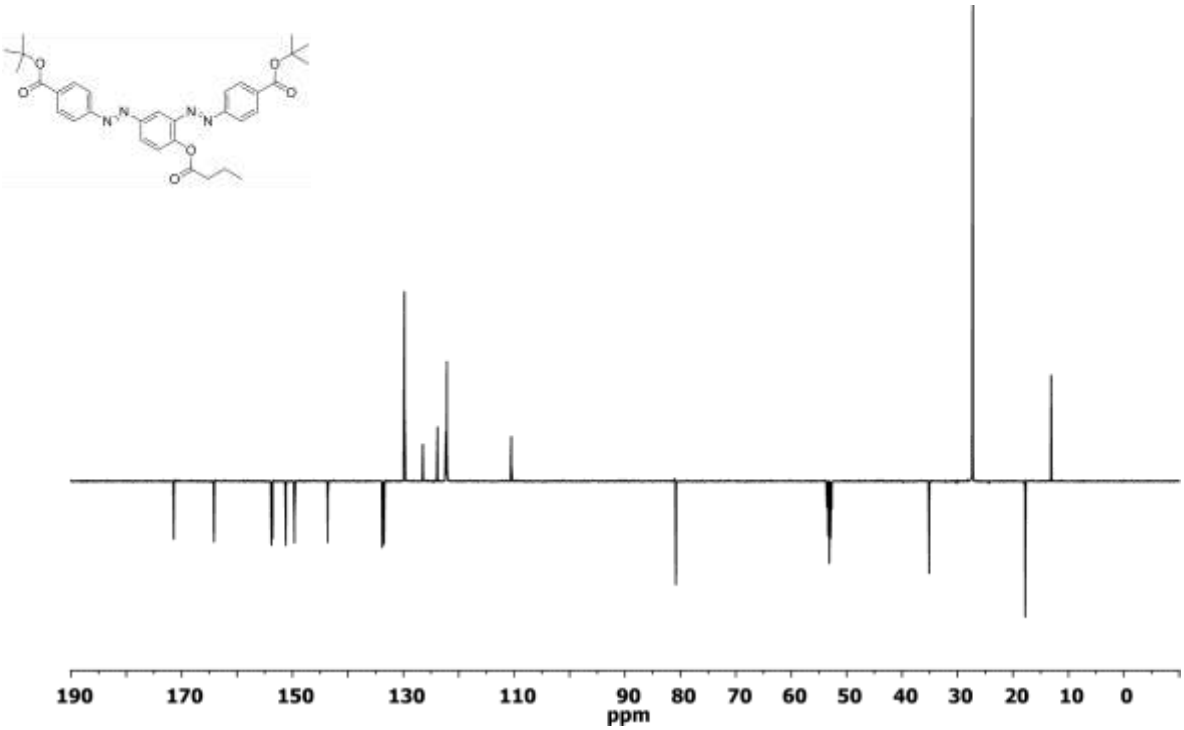

Fig. S9 APT ^{13}C-NMR spectrum of switch *E,E*-**2** in CD_2Cl_2.

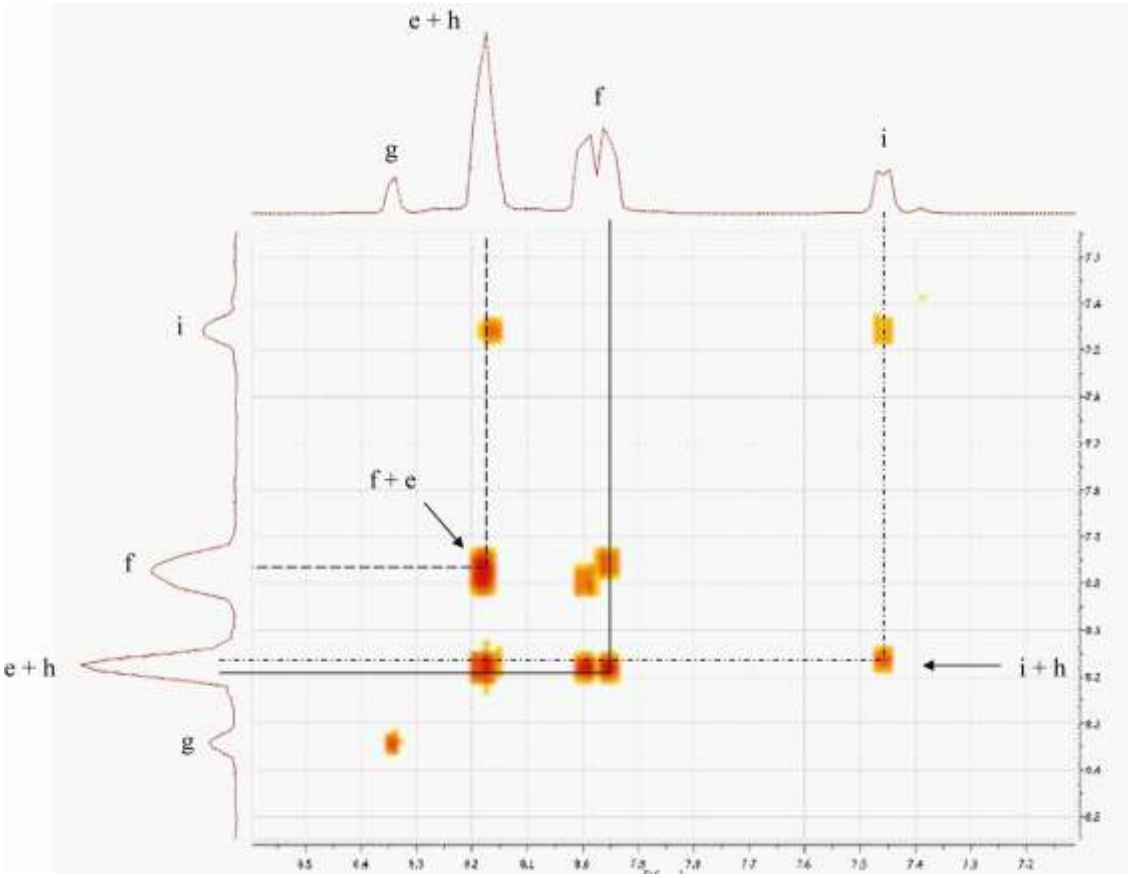

Fig. S10 Aromatic region of 2D GCOSY NMR spectrum of switch *E,E*-**2** in CD_2Cl_2.

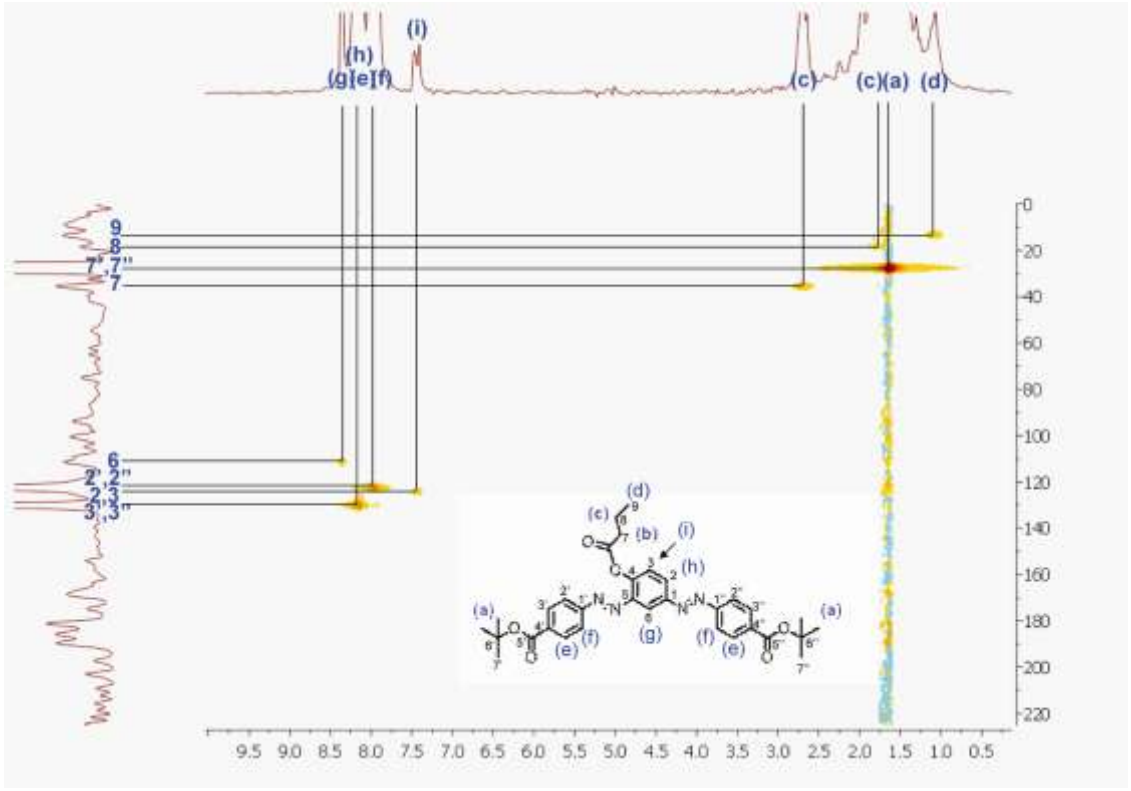

Fig. S11 2D HSQC NMR spectrum of switch *E,E*-**2** in CD_2Cl_2

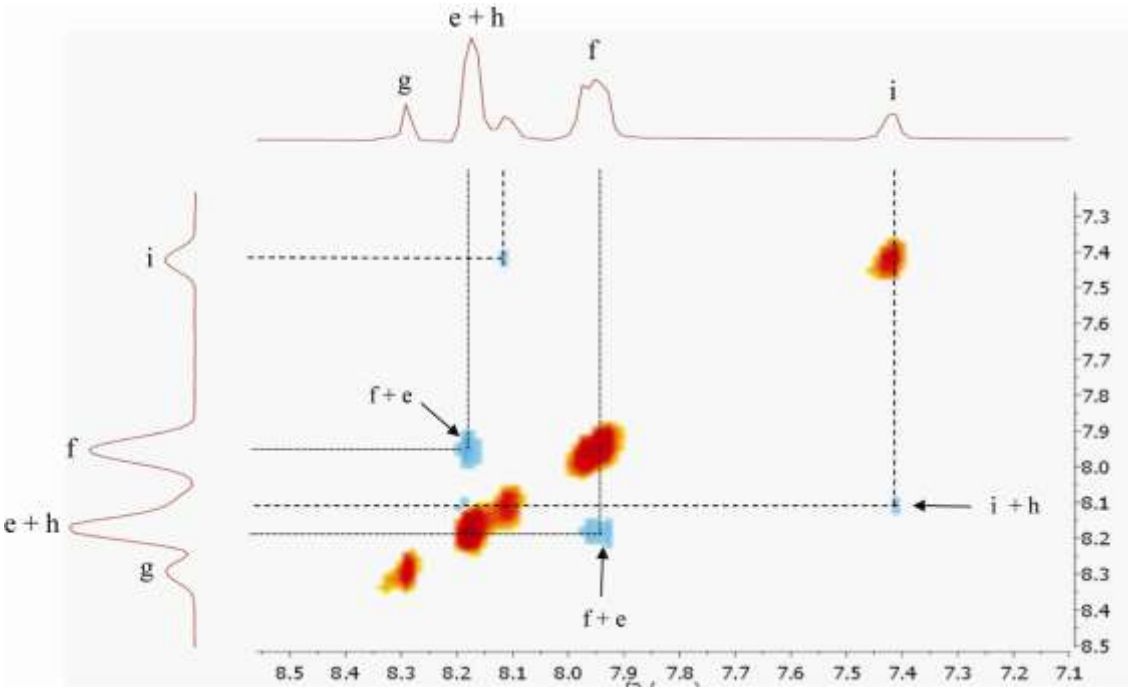

Fig. S12 2D ROESY NMR spectrum of switch *E,E*-**2** in CD_2Cl_2

2.5 Photochemical investigation of switch 3

The photochemical properties of bisazobenzene switch **3** were studied by UV/Vis spectroscopy. Irradiation (λ_{exc} 355 nm, at 20°C) of a solution of **3** in acetonitrile (3.87×10^{-5} M) did not result in changes in the UV/Vis spectrum (Fig. S13). This is probably due to the phenol substituent on the central phenyl ring. The azo-double bond in this case can be drawn as a single bond via resonance.[1] The photochemical properties were further investigated under basic (to increase electron donation) and acidic conditions (to limit electron donation).

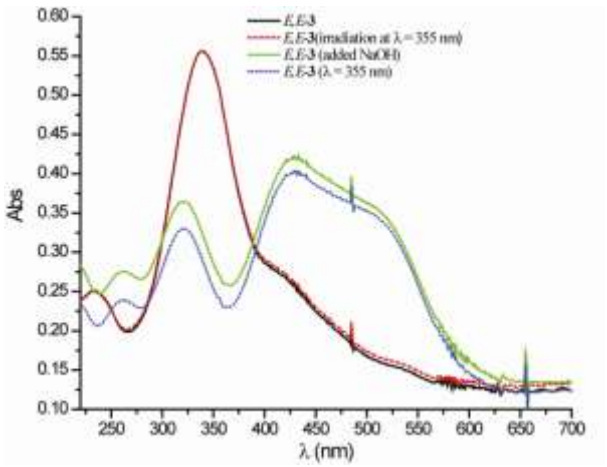

Fig. S13 Changes in the UV/Vis absorption spectra of *E*-**3** in acetonitrile (3.87×10^{-5} M) upon irradiation to PSS (λ_{exc} 365 nm at 20°C). *E*-**3** (——), *E*-**3** irradiated λ_{exc} 355nm (-----), *E*-**3** deprotonated using NaOH (——) and *E*-**3** irradiated λ_{exc} 355nm under basic conditions (·····).

Addition of NaOH to deprotonate the phenol moiety let to a red shift in the UV/Vis spectrum (Fig. S13). The band at λ_{max} 345 nm disappears and two new bands at 325 nm and 430 nm appear. Irradiation at λ_{exc} 355 and 455 nm did not lead to significant changes in the UV/Vis spectrum (Fig. S13). To exclude irreversible phenol oxidation under basic conditions NaOH was added to a solution of **3**, subsequently perchloric acid was added to reprotonate the phenol. The UV/Vis spectrum of **3** reverted to its initial shape (Fig. S14). Irradiation of the acidic solution of **3** let did not result in changes in the UV/Vis absorption spectrum.

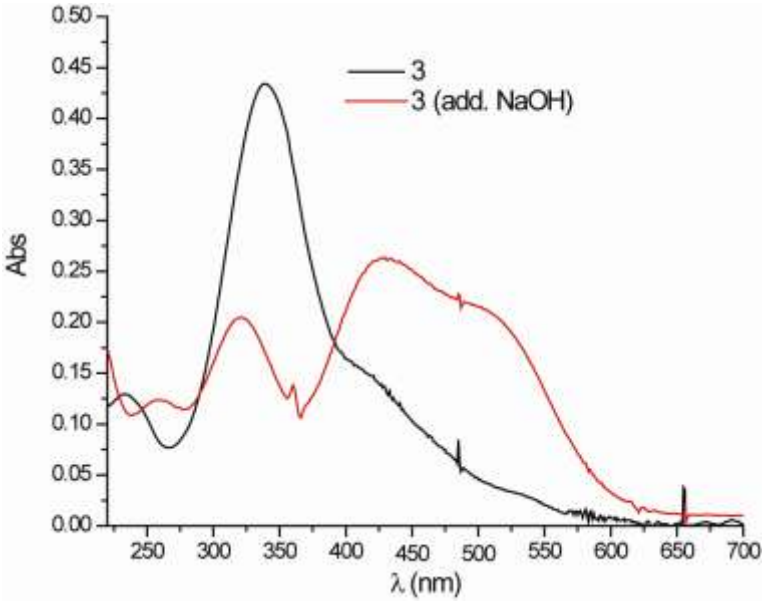

Fig. S14 Photochemical behaviour of switch **3** under acidic conditions studied by UV/Vis spectroscopy in acetonitrile at 20°C. *E*-**3** (——), *E*-**3** deprotonated using NaOH (——), *E*-**3** deprotonated using NaOH and subsequently protonated with perchloric acid (-----) and *E*-**3** irradiated λ_{exc} 355nm under acidic conditions (·····).

2.6 Identification of the PSS mixture of switch 2

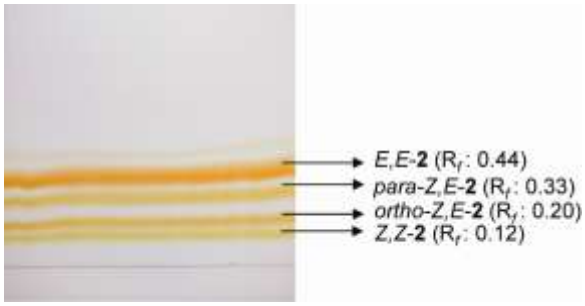

Fig. S15 PTLC chromatography of a PSS mixture of switch **2**. PLC: SiO_2 eluted with pentane/ethyacetate (10:1).

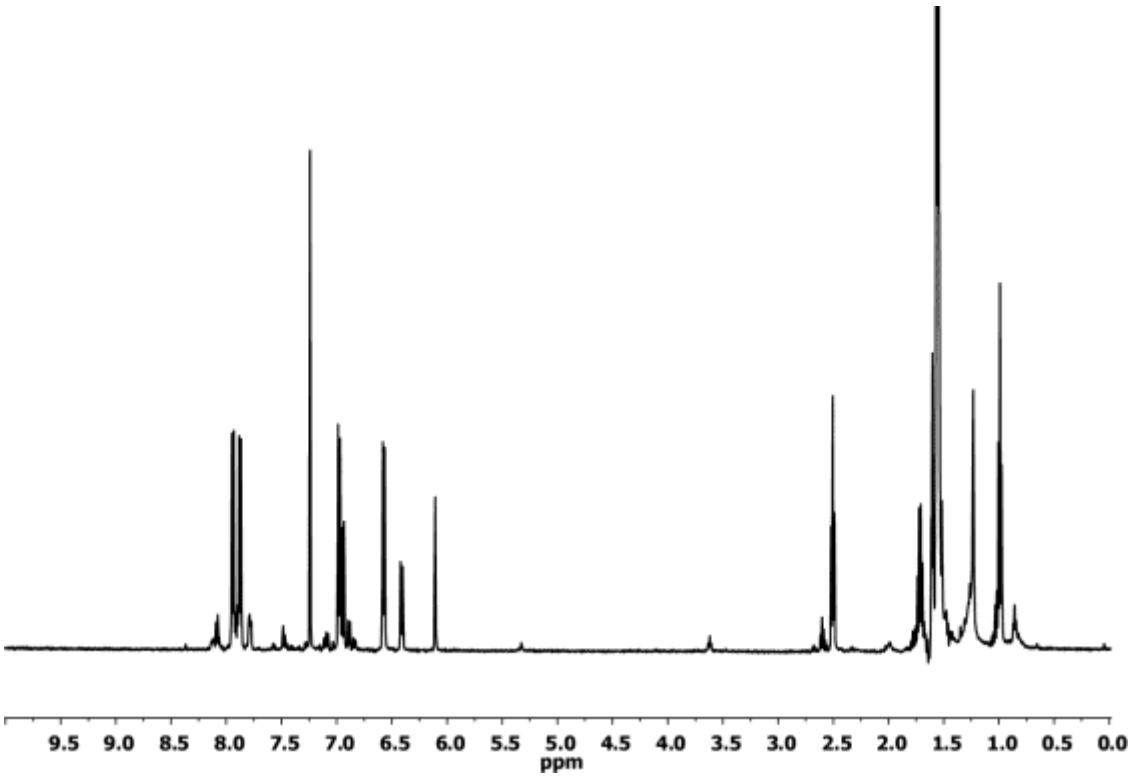

Fig. S16 ^{1}H-NMR spectrum of *Z,Z*-**2**, isolated by PTLC chromatography (R_f: 0.12). Sample contains small amount of the *para-Z,E*, *ortho-Z,E* and *E,E* isomers.[2]

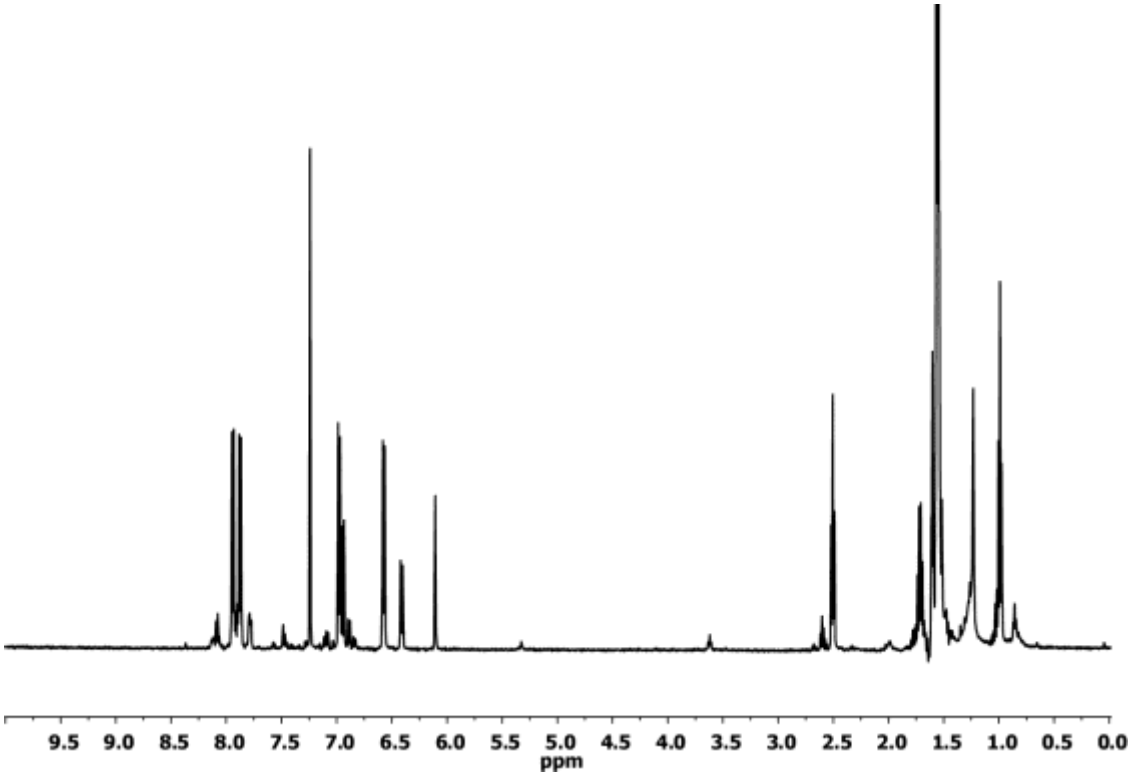

Fig. S17 ^{1}H-NMR spectrum of *para-Z,E*-**2**, isolated by PTLC chromatography (R_f: 0.33). Sample contains an equal amount of the *E,E* isomer.[2]

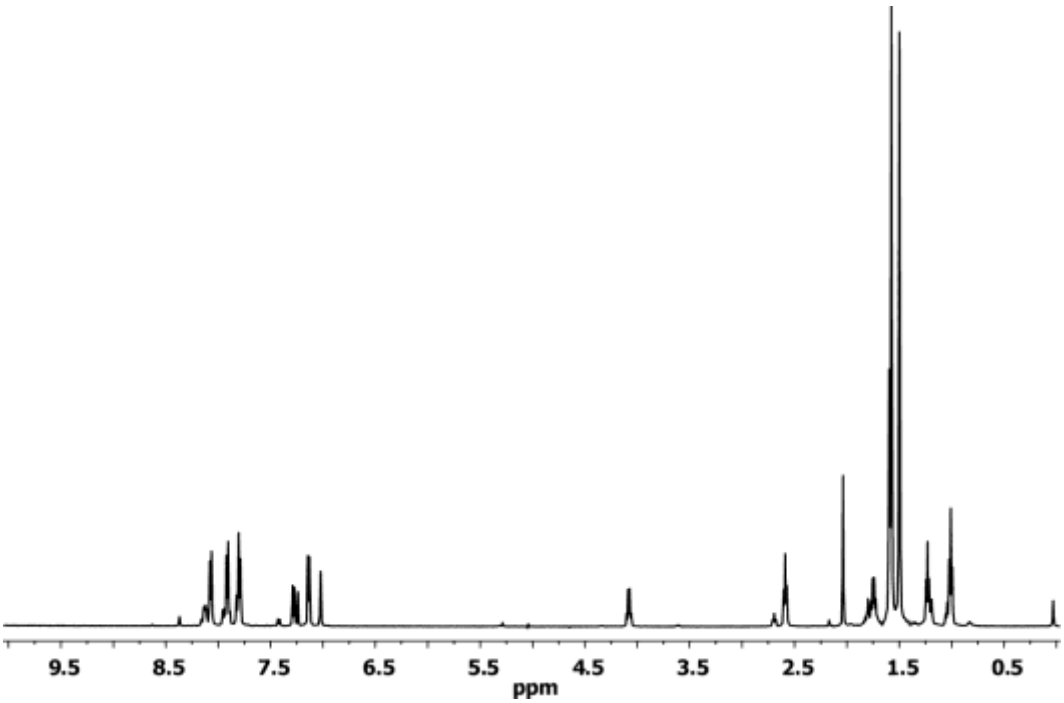

Fig. S18 ^{1}H-NMR spectrum of *ortho-Z,E*-**2**, isolated by PTLC chromatography (R_f: 0.20). Sample contains small amount of the *E,E* isomer.[2]

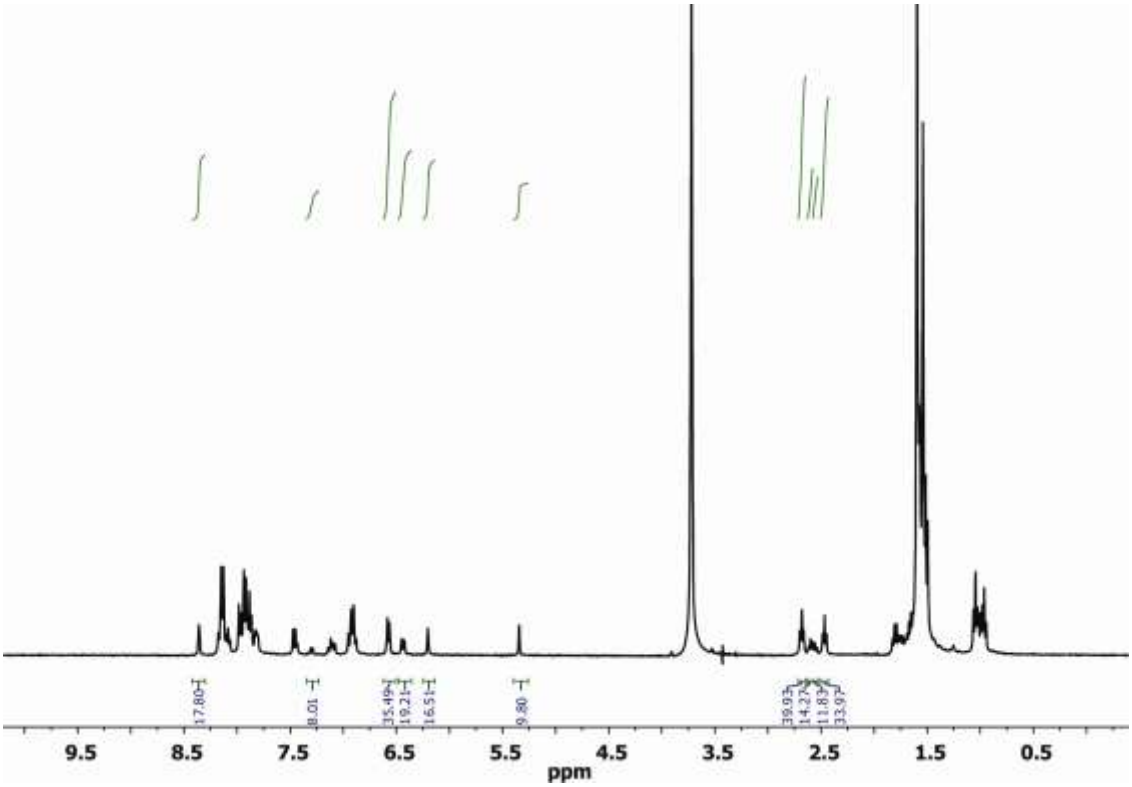

Fig. S19 ^{1}H-NMR spectrum of PSS mixture of **2**.

2.7 Calculated NMR spectra

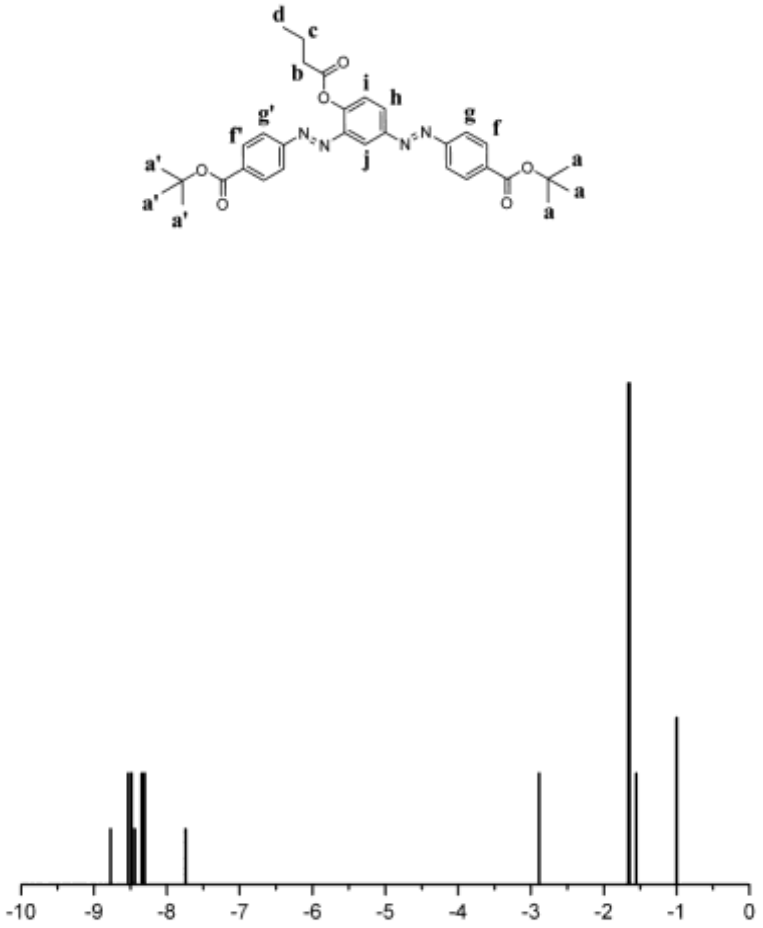

Fig. S20 Calculated ^{1}H-NMR spectra of *E,E*-**2** in $C_2D_4Cl_2$.

	chemical shift	intensity	referenced chemical shift	label
tBu	29.9737	9	-1.6488	a’
Ph	23.0917	2	-8.5309	f’
Ph	23.3158	2	-8.3068	g’
tBu	29.9591	9	-1.6634	a
Ph	23.1359	2	-8.4867	f
Ph	23.2788	2	-8.3438	g
Me	30.6226	3	-1.0000	d
CH_2	30.0676	2	-1.5550	c
CH_2	28.7340	2	-2.8886	b
Ph	22.8479	1	-8.7747	j
Ph	23.8808	1	-7.7418	i
Ph	23.1809	1	-8.4417	h

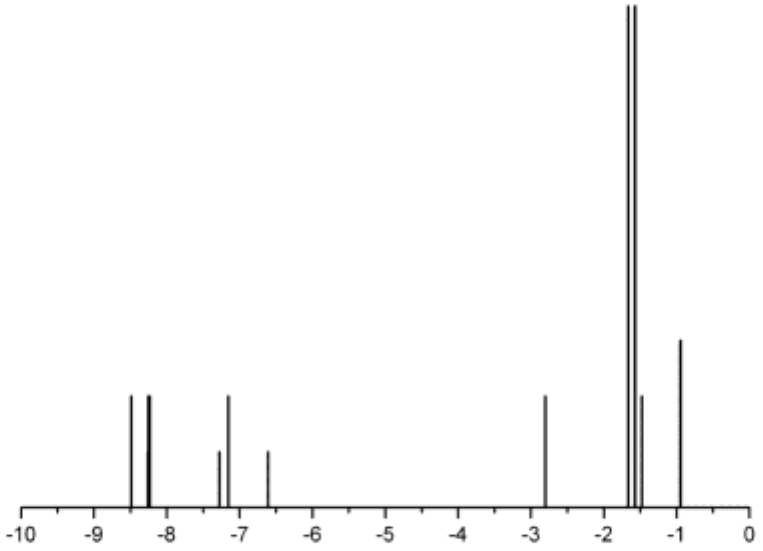

Fig. S21 Calculated ^{1}H-NMR spectra of *para*-*Z*,*E*-**2** in $C_2D_4Cl_2$.

	chemical shift	intensity	referenced chemical shift	label
tBu	29.9581	9	-1.6645	a’
Ph	23.1344	2	-8.4882	f’
Ph	23.3685	2	-8.2541	g’
tBu	30.0509	9	-1.5716	a
Ph	23.3905	2	-8.2321	f
Ph	24.4676	2	-7.1550	g
Me	30.6738	3	-0.9488	d
CH_2	30.1451	2	-1.4775	c
CH_2	28.8198	2	-2.8028	b
Ph	23.3638	1	-8.2588	j
Ph	24.3413	1	-7.2813	i
Ph	25.0126	1	-6.6100	h

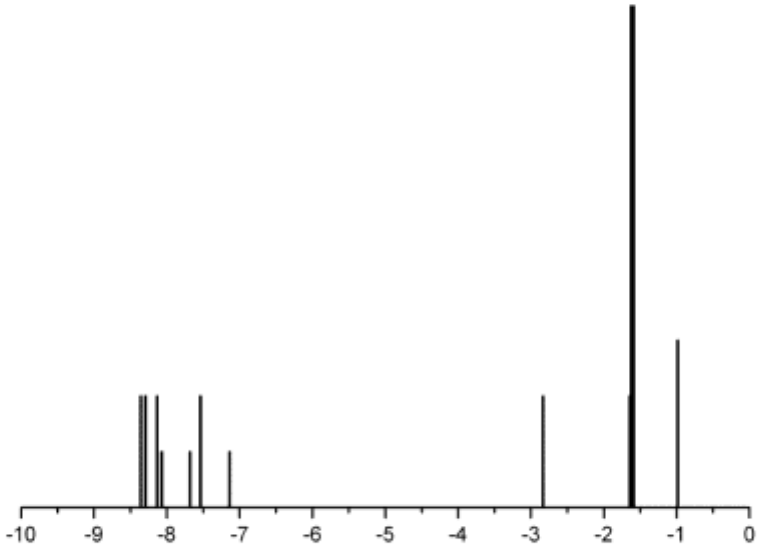

Fig. S22 Calculated ^{1}H-NMR spectra of *ortho-Z,E*-**2** in $C_2D_4Cl_2$.

	chemical shift	intensity	referenced δ (ppm)	label
tBu	30.0351	9	-1.5875	a’
Ph	23.3268	2	-8.2958	f’
Ph	24.0835	2	-7.5391	g’
tBu	29.9989	9	-1.6236	a
Ph	23.2608	2	-8.3618	f
Ph	23.4880	2	-8.1346	g
Me	30.6343	3	-0.9883	d
CH_2	29.9793	2	-1.6433	c
CH_2	28.7883	2	-2.8343	b
Ph	24.4809	1	-7.1417	j
Ph	23.9400	1	-7.6826	i
Ph	23.5529	1	-8.0697	h

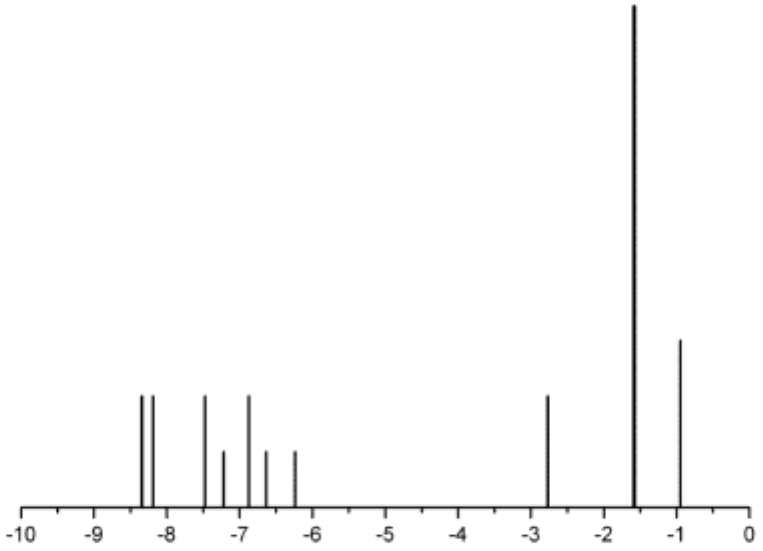

Fig. S23 Calculated ^{1}H-NMR spectra of *Z,Z*-**2** in $C_2D_4Cl_2$.

	chemical shift	intensity	referenced chemical shift	label
tBu	30.0316	9	-1.5910	a’
Ph	23.2790	2	-8.3436	f’
Ph	24.1470	2	-7.4756	g’
tBu	30.0473	9	-1.5752	a
Ph	23.4326	2	-8.1900	f
Ph	24.7503	2	-6.8723	g
Me	30.6705	3	-0.9520	d
CH_2	30.0408	2	-1.5818	c
CH_2	28.8535	2	-2.7691	b
Ph	24.9874	1	-6.6352	j
Ph	24.4011	1	-7.2215	i
Ph	25.3837	1	-6.2389	h

2.8 ESP calculations

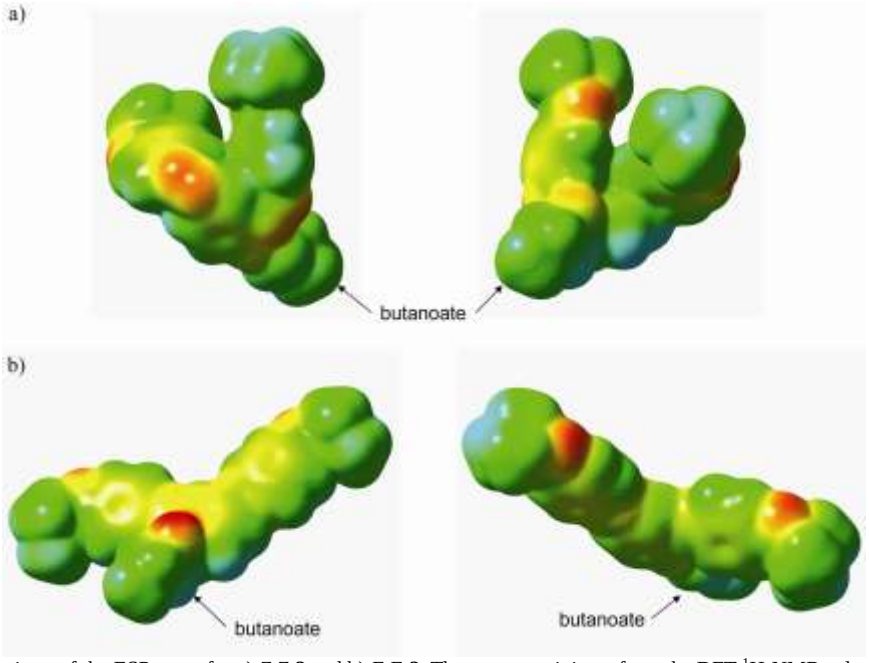

Fig. S24 Front and rear views of the ESP maps for a) *Z,Z*-**2** and b) *E,E*-**2**. These maps originate from the DFT ^{1}H-NMR calculations and were drawn with an isovalue of 0.0002.

2.9 Thermal behaviour of *Z* to *E* isomerisation of switch 2

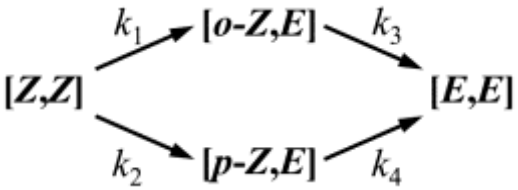

Fig. S25 Schematic representation of the possible pathways for thermal relaxation from unstable isomer *Z,Z*-**2** to *E,E*-**2**.

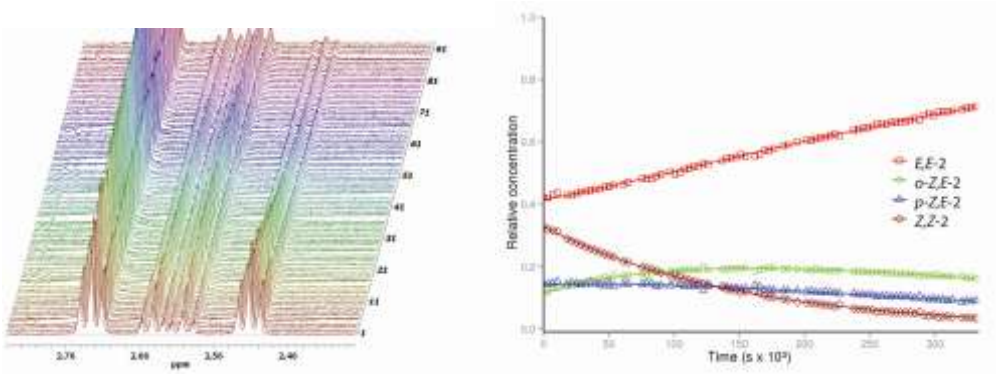

Fig. S26 a) ^{1}H-NMR spectroscopic thermal array of unstable isomers *Z,Z*-**2**, *para*-*Z,E*-**2** and *ortho*-*Z,E*-**2** at 28.16°C. b) Kinetic traces of thermal reversal of PSS mixture at 28.16°C, absorption by ^{1}H-NMR spectroscopy. *E,E*-**2** (□), *o*-*Z,E*-**2** (○), *p*-*Z,E*-**2** (△) and *Z,Z*-**2** (◇).

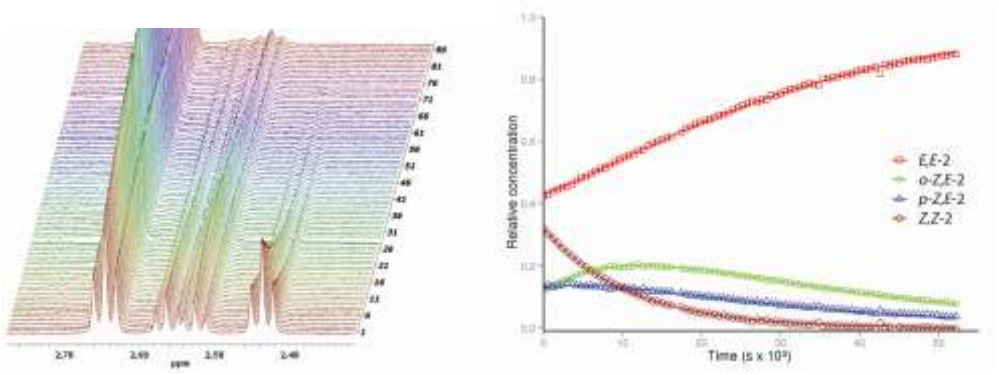

Fig. S27 a) ^{1}H-NMR spectroscopic thermal array of unstable isomers *Z,Z*-**2**, *para*-*Z,E*-**2** and *ortho*-*Z,E*-**2** at 49.03°C. b) Kinetic traces of thermal reversal of PSS mixture at 49.03°C, absorption by ^{1}H-NMR spectroscopy. *E,E*-**2** (□), *o*-*Z,E*-**2** (○), *p*-*Z,E*-**2** (△) and *Z,Z*-**2** (◇).

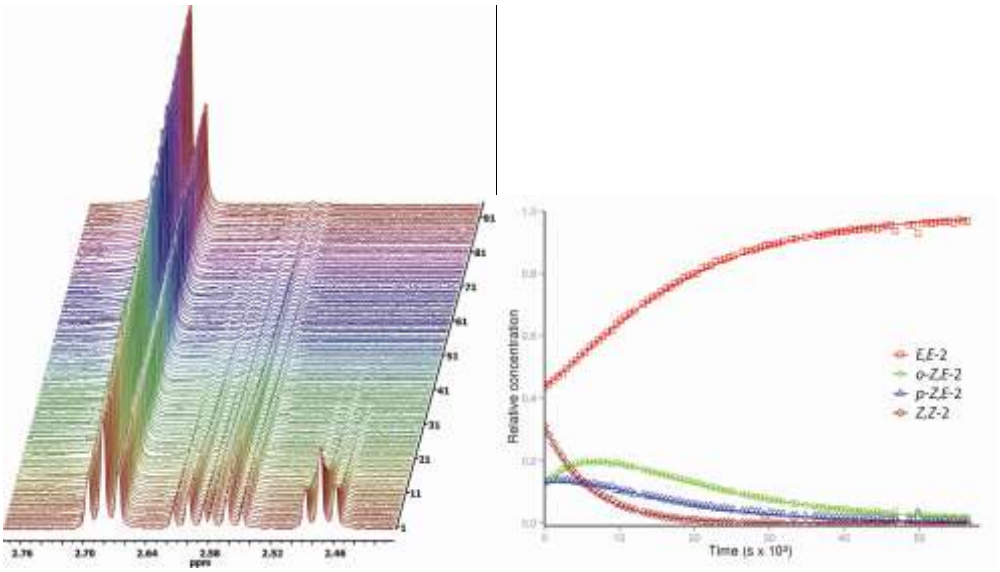

Fig. S28 a) ^{1}H-NMR spectroscopic thermal array of unstable isomers *Z,Z*-**2**, *para*-*Z,E*-**2** and *ortho*-*Z,E*-**2** at 54.51°C. b) Kinetic traces of thermal reversal of PSS mixture at 54.51°C, absorption by ^{1}H-NMR spectroscopy. *E,E*-**2** (□), *o*-*Z,E*-**2** (○), *p*-*Z,E*-**2** (△) and *Z,Z*-**2** (◇).

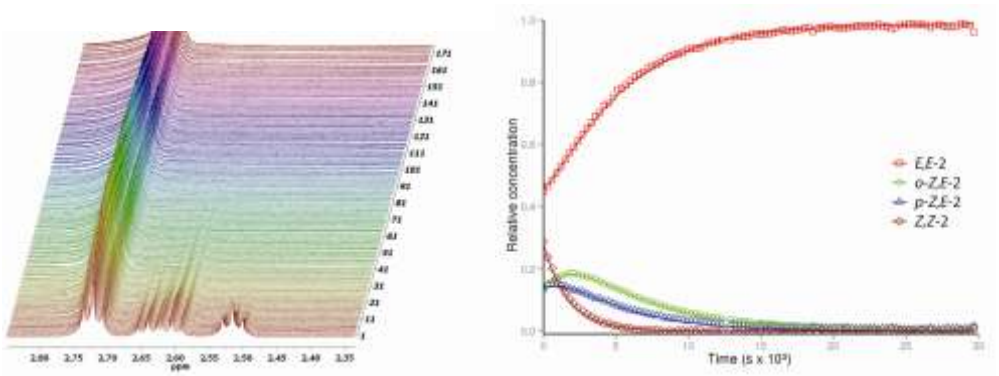

Fig. S29 a) ^{1}H-NMR spectroscopic thermal array of unstable isomers *Z,Z*-**2**, *para*-*Z,E*-**2** and *ortho*-*Z,E*-**2** at 64.61°C. b) Kinetic traces of thermal reversal of PSS mixture at 64.61°C, absorption by ^{1}H-NMR spectroscopy. *E,E*-**2** (□), *o*-*Z,E*-**2** (○), *p*-*Z,E*-**2** (△) and *Z,Z*-**2** (◇).

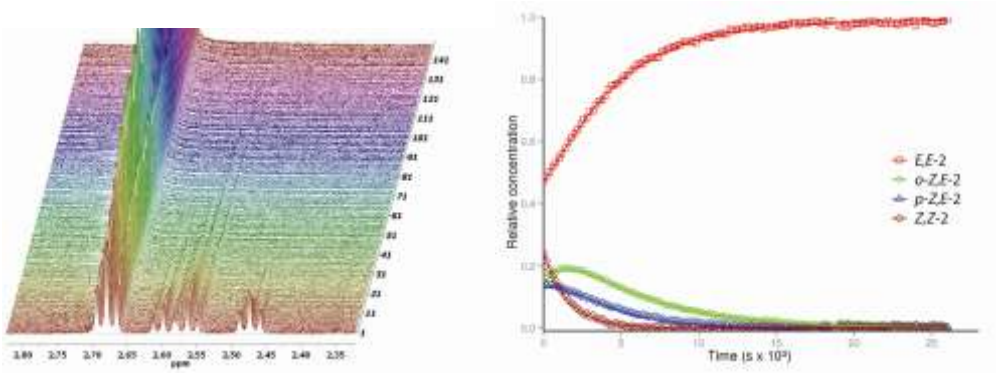

Fig. S30 a) ^{1}H-NMR spectroscopic thermal array of unstable isomers *Z*,*Z*-**2**, *para*-*Z*,*E*-**2** and *ortho*-*Z*,*E*-**2** at 68.71°C. b) Kinetic traces of thermal reversal of PSS mixture at 68.71°C, absorption by ^{1}H-NMR spectroscopy. *E*,*E*-**2** (□), *o*-*Z*,*E*-**2** (○), *p*-*Z*,*E*-**2** (△) and *Z*,*Z*-**2** (◇).

2.10 Fitting model for the kinetic analysis of thermal *Z* to *E* isomerisation of switch 2

Our aim was to extract the four rate constants for *Z* to *E* isomerisation of the thermally unstable isomers of switch **2** from the kinetic traces in Fig. S26-S30. Each of the four kinetic traces was described by two rate constants, as shown in Fig. S25. The four species *Z*,*Z*-**2**, *o*-*Z*,*E*-**2**, *p*-*Z*,*E*-**2** and *E*,*E*-**2** are associated with state functions A(t), B(t), C(t) and D(t) respectively, which describes their relative concentration as a function of time. These functions depend on the rate constants k_i, as well as the initial concentrations $A(0) \equiv A_0$, $B(0) \equiv B_0$, etc. These functions were used to form the following set of differential equations:

$$\frac{dA(t)}{dt} \equiv A'(t) = -k_1 A(t) - k_2 A(t) \quad (1a)$$

$$\frac{dB(t)}{dt} \equiv B'(t) = k_1 A(t) - k_3 B(t) \quad (1b)$$

$$\frac{dC(t)}{dt} \equiv C'(t) = k_2 A(t) - k_4 C(t) \quad (1c)$$

$$\frac{dD(t)}{dt} \equiv D'(t) = k_3 A(t) - k_4 D(t) \quad (1d)$$

A solution was obtained using Laplace transforms. Given a function *f*(t), its Laplace transform can be written as.

$$L\ f(t) \equiv \tilde{f}(s) \equiv \int_0^\infty f(t) e^{-sx}\, dt \quad (2)$$

The Laplace transformations have the following properties:

$$L\ af(t) + bg(t) = aL\ f(t) + bL\ g(t) \quad (3)$$

and

$$L\left[\frac{df(t)}{df}\right] = sL\ f(t) - f(0) \quad (4)$$

Taking the Laplace transforms of this set of differential equations and using equation 4, one obtains an ordinary set of equations in s-space. These resultant equations are solved and their solutions transformed back to the time domain.

$$K_1 = \frac{k_1}{k_1 + k_2 - k_3} \tag{5a}$$

$$K_2 = \frac{k_2}{k_1 + k_2 - k_4} \tag{5b}$$

The solution of the set of differential equations are written as:

$$A(t) = A_0 e^{-(k_1+k_2)t} \tag{6a}$$

$$B(t) = B_0 + K_1 A_0 e^{-k_3 t} - K_1 A_0 e^{-(k_1+k_2)t} \tag{6b}$$

$$C(t) = C_0 + K_1 A_0 e^{-k_4 t} - K_2 A_0 e^{-(k_1+k_2)t} \tag{6c}$$

$$D(t) = A_0 + B_0 + C_0 + D_0 - B_0 + K_1 A_0 e^{-k_3 t} - C_0 + K_2 A_0 e^{-k_4 t} + k_3 K_1 + k_4 K_2 \frac{A_0 e^{-(k_1+k_2)}}{(k_1 + k_2)} \tag{6d}$$

The model parameters were obtained by a least squares fit to the available data.

Table 1 Determined rate constant *k* for the thermal isomerisation pathways thermal *Z,Z*-2 to *E,E*-2 isomerisation at 28.16 °C

Rate constant *k* for thermal *Z* to *E*	Value *k*	Statistical error	Systematic error	Total error
k_1	4.811e-06	± 8.5e-08	± 1.7e-07	± 1.9e-07
k_2	1.840e-06	± 8.9e-08	± 2.3e-07	± 2.5e-07
k_3	2.814e-06	± 6.0e-08	± 2.3e-07	± 2.4e-07
k_4	3.232e-06	± 8.8e-08	± 3.9e-07	± 4.0e-07

Table 2 Determined rate constant *k* for the thermal isomerisation pathways thermal *Z,Z*-2 to *E,E*-2 isomerisation at 49.03°C

Rate constant *k* for thermal *Z* to *E*	Value *k*	Statistical error	Systematic error	Total error
k_1	6.762e-05	± 7.4e-07	± 3.4e-07	± 8.2e-07
k_2	2.527e-05	± 7.7e-07	± 6.2e-07	± 9.9e-07
k_3	3.459e-05	± 2.8e-07	± 6.1e-07	± 6.7e-07
k_4	4.034e-05	± 5.0e-07	± 5.0e-07	± 7.0e-07

Table 3 Determined rate constant *k* for the thermal isomerisation pathways thermal *Z,Z*-2 to *E,E*-2 isomerisation at 54.51°C

Rate constant *k* for thermal *Z* to *E*	Value *k*	Statistical error	Systematic error	Total error
k_1	1.176e-04	± 2.1e-06	± 8.4e-07	± 2.3e-06
k_2	5.174e-05	± 2.1e-06	± 8.0e-07	± 2.3e-06
k_3	5.842e-05	± 5.9e-07	± 4.1e-07	± 7.2e-07
k_4	7.755e-05	± 1.2e-06	± 6.2e-07	± 1.4e-06

Table 4 Determined rate constant *k* for the thermal isomerisation pathways thermal *Z,Z*-2 to *E,E*-2 isomerisation at 64.61°C

Rate constant *k* for thermal *Z* to *E*	Value *k*	Statistical error	Systematic error	Total error
k_1	3.750e-04	± 1.0e-05	± 1.8e-06	± 1.1e-05
k_2	2.022e-04	± 1.0e-05	± 5.6e-06	± 1.2e-05
k_3	1.896e-04	± 2.6e-06	± 2.1e-06	± 3.4e-06
k_4	2.361e-04	± 4.4e-06	± 2.0e-06	± 4.8e-06

Table 5 Determined rate constant *k* for the thermal isomerisation pathways thermal *Z,Z*-2 to *E,E*-2 isomerisation at 68.71°C

Rate constant *k* for thermal *Z* to *E*	Value *k*	Statistical error	Systematic error	Total error
k_1	3.997e-04	± 1.0e-05	± 6.4e-06	± 1.2e-05
k_2	2.355e-04	± 9.8e-06	± 1.3e-05	± 1.7e-05
k_3	1.965e-04	± 2.0e-06	± 3.5e-06	± 4.1e-06
k_4	3.191e-04	± 4.7e-06	± 7.6e-06	± 9.0e-06

The rate constants k1, k2, k3 and k4, are extracted from the fits at each of the temperatures (28, 49, 55, 65 and 69 °C respectively). The statistical error is set at 1σ as coming from the fit. We estimate the systematic error by varying the end time of the fit. As at high temperatures, the reaction proceeds more rapid than at the lower temperatures. Especially at 28 °C, the reaction has not been completed by the time the kinetic analysis is terminated. Since the termination time-point might influence the fitted coefficients. We attempt to estimate the systematic error as a result of the termination time of data collection, by a fit using various termination times. As can be expected we see that at higher temperatures the variation of the termination times of the fit has a relative small effect on the results of the fit.

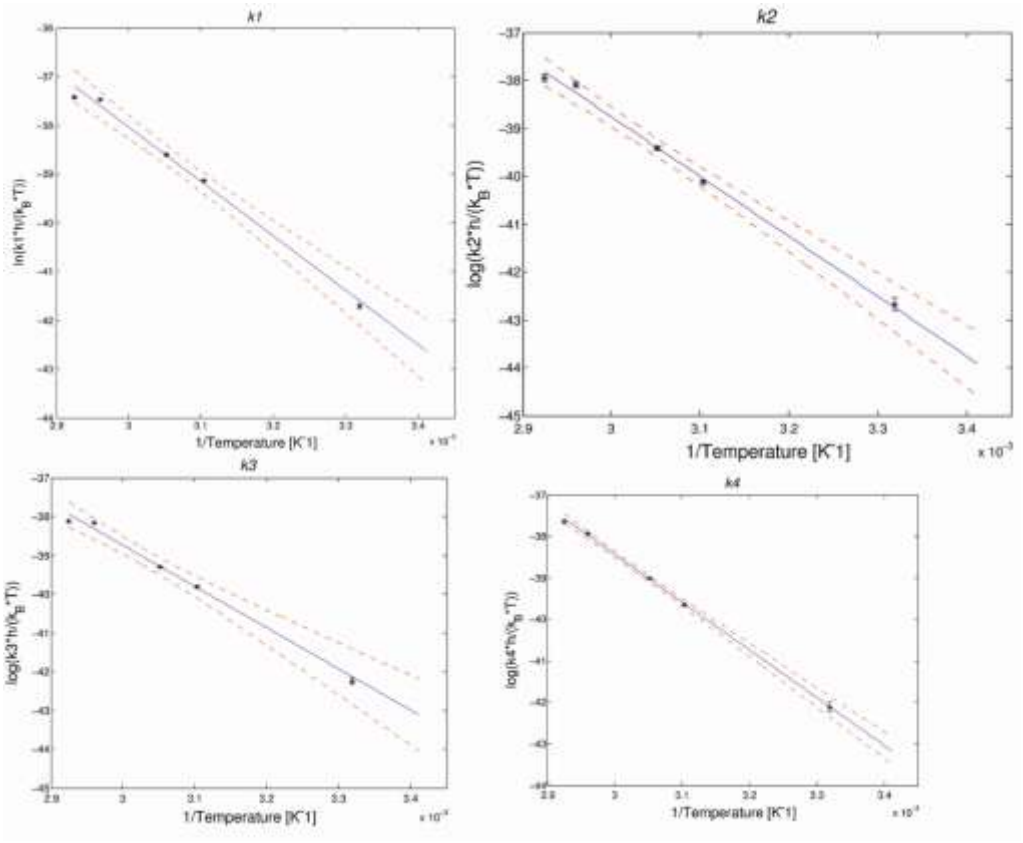

Fig. S31 Eyring plots for thermal *Z* to *E* isomerisation of **2**. a) *Z,Z* to *ortho-Z,E* b) *Z,Z* to *para-Z,E* c) *ortho-Z,E* to *E,E* and d) *para-Z,E* to *E,E*.

Notes and references

1 D. Escudero, S. Trupp, B. Bussemer, G. J. Mohr, and L. González, *J. Chem. Theory Comput.*, 2011, **7**, 1062.

2 Traces of ethyl acetate remain in the ^{1}H-NMR sample of ortho-Z,E-2 and para-Z,E-2 after thin layer chromatography (SiO_2, 1:10 ethyl acetate / pentane). The organic solvents were removed in vacuo (30°C), however due to the thermal Z to E isomerisation, the isomers cannot be heated under reduced pressure for an extended period. During removal of the organic solvent ortho-Z,E-**2** and para-Z,E-**2** partially revert back to the thermally stable E,E-**2** isomer.